Theoretical Study of Dynamics for the Abstraction Reaction H′ + HBr(v=0, j=0) → H′H + Br†

Wenqin Zhang, Shulin Cong, Cuihua Zhang, Xuesong Xu, and Maodu Chen*

School of Physics and Optoelectronic Technology, School of Chemical Engineering, College of Advanced Science and Technology, Dalian University of Technology, Dalian 116024, PR China

Received: December 2, 2008; Revised Manuscript Received: February 7, 2009

Theoretical studies of the dynamics of the abstraction reaction, H′ + HBr (v=0,j=0) → H′H + Br, have been performed with quasiclassical trajectory method (QCT) on a new ab initio potential energy surface (Y. Kurosaki and T. Takayanagi, private communication). The calculated QCT cross sections are in good agreement with earlier quantum wave packet results over most of the collision energy range from 0.1 to 2.6 eV, and the state-resolved rotational distributions of the product H′H molecule are quantitatively consistent with the experimental results. Comparisons of the QCT-calculated rotational-state-resolved cross sections on different potential energy surfaces show that the characteristics of the potential energy surface in the region far away from the minimum energy path have a large influence on the title abstraction reaction dynamics, and the indirect reactions that do not follow the minimum energy path have little influence on the differential cross sections (DCS). The DCSs are mainly governed by the direct reactions that do follow the minimum energy path, at both low and high collision energies. The degree of the rotational alignment of the product H′H molecule is strong at high collision energies, which means that the influence of the indirect reactions on the product rotational alignment is negligible, whereas the distribution of $P(\phi_r)$ is sensitive to the indirect reactions at high collision energies. With increasing collision energy, the polarization of the product rotational angular momentum decreases and the molecular rotation of the product prefers an in-plane reaction mechanism rather than the out-of-plane mechanism.

1. Introduction

The H + HBr reaction, along with other reactions of atomic hydrogen with hydrogen halides such as the FH_2 and ClH_2 reactive systems,[1−7] has been of fundamental importance in the development of chemical kinetics and reaction dynamics. The experimental studies on the abstraction reaction, H′ + HBr → H′H + Br, and the exchange reaction, H′ + HBr → H′Br + H, have been mainly focused on the determination of reaction rates and kinetic isotope effects.[8−10] The abstraction reaction, H′ + HBr → H′H + Br, is an extreme example of the mass combination light + light-heavy → light-light + heavy. This combination causes the skew angle in the H + HBr mass-weighted coordinate system to be $\beta = 45°$.[11] This kinematic feature suggests that about one-half ($\cos^2 \beta$) of the incident translational energy is unavailable for internal excitation of the products. Such a situation is referred to as "kinematically constrained". However, Zare and co-workers presented experimental evidence that a small fraction of the H′ + HBr reactive trajectories did not obey this kinematic constraint and formed the H′H product with highly excited rotational states.[12] On the basis of quasiclassical trajectory (QCT) calculations on an e-LEPS potential energy surface (PES), they proposed two distinct mechanisms: a direct reactive mechanism in which the H′H product recoils away immediately, and an indirect reactive mechanism in which the H′ atom suffers several collisions with the HBr molecule before the H′H product is formed. H′H products with low internal excitation, whose distributions are limited by the skew angle β, are formed almost exclusively from direct trajectories that have an almost perfectly collinear at the transition state, whereas H′H products with high internal excitation are formed mainly from indirect trajectories with bent transition states. Reactions at high collision energies are not required to stay near the minimum energy path. Reaction paths that deviate far from the minimum energy path are more common than that previously expected, and have also been observed in the photodissociation of formaldehyde to form H_2 and CO[13] and the reaction O + HCl → ClO + H.[14] Panda et al.[15] reported quantum mechanical (QM) calculations for the H′ + HBr(v=j=0) → H′H($v′$,$j′$) + Br reaction on the e-LEPS PES at collision energies (E_c) in the range 2.1−2.5 eV, and they found that the calculated product rotational distributions showed good agreement with the previous experimental results and QCT predictions.

Although abstraction reactions of the type H′ + HX → H′H + X, where X = F, Cl, Br, have similar kinematics, their dynamics may be different as a result of differences in the potential energy surfaces.[16] An accurate potential energy surface for the BrH_2 system has been difficult to achieve. A decade ago, Lynch et al. carried out multireference configuration interaction (MRCI) calculations with a large basis set for the ground-state PES for the BrH_2 system at 104 geometries preselected for convenient use in fitting an analytical PES via the extended LEPS function form with a three-center term.[17] The calculated rate constants for the abstraction and exchange reactions on this PES were found to be remarkably smaller than the experimentally observed values.[8−10] Recently, Tang and co-workers[18−20] carried out quantum time-dependent wave packet calculations for the Br + H_2 reaction on new ab initio potential energy surfaces, named MB1,[21] MB2,[22] MB3,[23] and

† Part of the "George C. Schatz Festschrift".

* Corresponding authors. E-mail: mdchen@dlut.edu.cn.

10.1021/jp8105716 CCC: $40.75
Published on Web 03/16/2009

the MB3 PES was suggested to be more accurate than the e-LEPS, MB1 and MB2 PESs.

Most of the previous work in reaction dynamics has focused on scalar properties such as the rate constant, cross section, product population distribution, etc. However, complete information on the forces acting in the reaction also requires a consideration of vector properties, as they are key indicators of the anisotropy of the potential energy surface involved in the reaction.[24−26] Hence, a complete understanding of the gas-phase reaction dynamics is only possible after accounting for both scalar and vector properties together.[25,27−29] In a prescient series of papers published in the mid 1970s to early1980s, Herschbach and co-workers attempted to persuade reaction dynamicists that "the analysis of angular momentum orientation or polarization in molecular scattering processes provides a powerful method for characterizing the collision dynamics and potential energy surfaces."[30−33] One aspect of this polarization is the correlation between reactant and product relative velocity vectors, the $\mathbf{k}-\mathbf{k}'-\mathbf{j}'$ correlation, which provides information otherwise lost by averaging over the random azimuthal orientation of impact parameters.[33] To gain more insight into the detailed dynamics of the title abstraction reactions, we have carried out quasiclassical trajectory calculations for the H′ + HBr(v=j=0) → H′H + Br reaction in the collision energy range 0.1−2.6 eV, and we have studied the vector correlations. The paper is organized as follows: Section 2 provides a brief review of the theoretical methodologies. Section 3 presents and discusses the calculated results. The main results and conclusions are summarized in section 4.

2. Computational Methods

A. Rotational Polarization of the Product. The center-of-mass (CM) frame is utilized in the calculations. The z-axis lies in the direction of the reagent relative velocity $\mathbf{k}$, whereas the y-axis is perpendicular to the xz plane containing $\mathbf{k}$ and $\mathbf{k}'$. θ is the angle between the reagent relative velocity and product relative velocity (so-called scattering angle), corresponding to the angle between $\mathbf{k}$ and $\mathbf{k}'$. θ_r and ϕ_r are the polar and azimuthal angles of the final rotational angular momentum $\mathbf{j}'$. The full three-dimensional angular distribution associated with $\mathbf{k}$, $\mathbf{k}'$, and $\mathbf{j}'$ is represented with a set of generalized polarization-dependent differential cross sections (PDDCS) in the CM frame.[32−34] The fully correlated CM angular distribution is written as the sum

$$P(\omega_t, \omega_r) = \sum_{kq} \frac{[k]}{4\pi} \frac{1}{\sigma} \frac{d\sigma_{kq}}{d\omega_t} C_{kq}(\theta_r, \phi_r) \quad (1)$$

where $[k] = 2k + 1$, $1/\sigma(d\sigma_{kq}/d\omega_t)$ is a generalized polarization-dependent differential cross section (PDDCS), and $C_{kq}(\theta_r,\phi_r)$ are modified spherical harmonics. The differential cross-section is given by

$$\frac{1}{\sigma} \frac{d\sigma_{00}}{d\omega_t} = P(\omega_t) = \frac{1}{4\pi} \sum_{k_1} [k_1] h_0^{k_1}(k_1, 0)\, P_{k_1}(\cos\theta_t) \quad (2)$$

The bipolar moments $h_0^{k_1}(k_1,0)$ are evaluated using the expectation values of the Legendre moments of the differential cross-section,

$$h_0^{k_1}(k_1, 0) = \langle P_{k_1}(\cos\theta_t)\rangle \quad (3)$$

The usual two vector correlation ($\mathbf{k}-\mathbf{j}'$) is expanded in a series of Legendre polynomials, and the distribution $P(\theta_r)$ can be written as[25,26,35,36]

$$P(\theta_r) = \frac{1}{2} \sum_k (2k + 1) a_0^{(k)} P_k(\cos\theta_r) \quad (4)$$

where

$$a_0^{(k)} = \int_0^{\pi} P(\theta_r)\, P_k(\cos\theta_r) \sin\theta_r\, d\theta_r = \langle P_k(\cos\theta_r)\rangle \quad (5)$$

The coefficients $a_0^{(k)}$ are called orientation (k is odd) or alignment (k is even) parameters. $k = 2$ indicates the product rotational alignment:[37]

$$a_0^{\,2} = \langle P_2(\cos\theta_r)\rangle = \langle P_2(\mathbf{j}'\cdot\mathbf{k})\rangle = \frac{1}{2}\langle 3\cos^2\theta_r - 1\rangle \quad (6)$$

Here we only calculate the average rotational alignment of the product, as it has been measured in most experiments to date. In the work reported in this article, $P(\theta_r)$ is expanded up to k = 18, which shows good convergence.

The dihedral angle distribution function $P(\phi_r)$ describing $\mathbf{k}-\mathbf{k}'-\mathbf{j}'$ correlation can be expanded in Fourier series as[25,26,35,36]

$$P(\phi_r) = \frac{1}{2\pi}\left(1 + \sum_{\text{even},n>2} a_n \cos n\phi_r + \sum_{\text{odd},n\geq 1} b_n \sin n\phi_r\right) \quad (7)$$

where

$$a_n = 2\langle\cos n\phi_r\rangle \qquad \text{and} \qquad b_n = 2\langle\sin n\phi_r\rangle \quad (8)$$

In the calculations, $P(\phi_r)$ is expanded up to n = 24, which shows good convergence.

B. Potential Energy Surface. To further improve the PES presented by Lynch et al.,[17] Kurosaki and Takayanagi constructed a series of global adiabatic potential energy surfaces of the lowest three doublet states ($1^2A'$, $2^2A'$, and $1^2A''$) for the BrH_2 system, named MB1,[21] MB2,[22] and MB3,[23] using the multireference configuration interaction method. The Davidson correction with the aug-cc-pVTZ basis set and the spin−orbit coupling and the diabatization of the two $^2A'$ PESs are included in the calculations. To obtain a better description of the long-range forces, the spin−orbit (SO) coupling effect has been considered in the two-body terms in the potential function, but somewhat unsatisfactory agreement still remains with experimental observations. The fit on the MB3 PES modified the arbitrary well at the T-shape geometry on the MB2 PES and replaced it with a barrier. Figure 1 shows the contour plots of the MB3 PES. The barrier height of the title abstraction reaction on this new PES is 0.066 eV at collinear geometry and 0.916 eV at the T-shaped geometry. Because the transition-state geometry is very close to this collinear configuration, the left plot in Figure 1 represents the minimum energy path for the reaction, H′ + HBr → H′H + Br. The collinear configurations on the MB3 PES are similar to those on the e-LEPS PES in this region, and the barrier heights are almost identical. For the T-shaped configurations, the differences between the MB3 and e-LEPS PESs become fairly large. The barrier height at

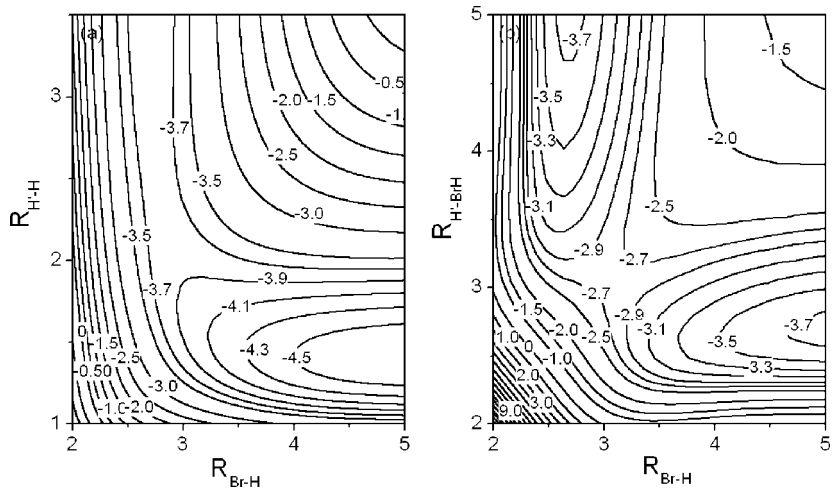

Figure 1. Contour plots of the MB3 potential energy surface (a) for the collinear configuration H′−H−Br and (b) for the T-shape configuration H′−Br−H. Energies are given in electronvolts (eV) with respect to the H′ + HBr asymptote.

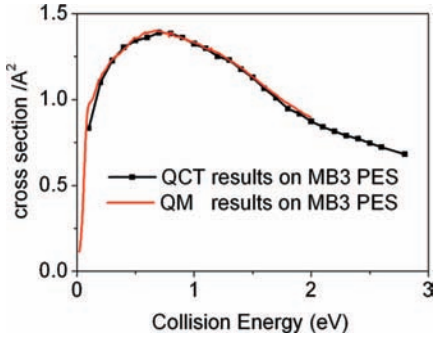

Figure 2. Comparison between the QCT-computed cross sections (the solid line with square) in this work and the previous QM-computed cross section (the solid line) for the H′ + HBr(v=0,j=0) → H′H + Br reaction. The QM results are taken from ref 39.

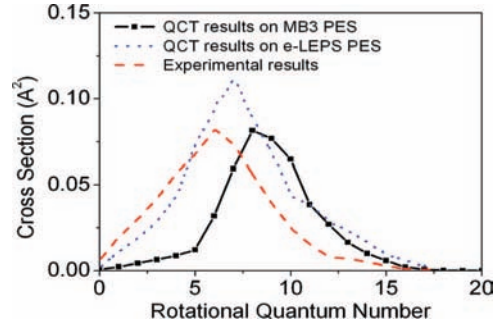

Figure 3. Comparison between the QCT-computed cross section (the solid line with square) and another theoretical cross section for the chemical reaction, H′ + HBr(v=0,j=0) → H′H(v'=2,j) + Br, at a collision energy of 2.3 eV. The experimental results (the dashed line) from ref 12 are also included. The experimental results have been normalized to match the present QCTs because only relative cross-sections were measured. The dotted line is the QCT results of Zare and co-workers on the e-LEPS PES (also from ref 12), and the cross sections are multiplied by a factor of 10.

T-shaped configurations on the MB3 PES is 0.11 eV lower than that on the e-LPES PES. According to the quantum time-dependent wave packet calculations by the Tang group[18−20] for Br + H_2 reaction on these new PESs, the MB3 PES is suggested to be more reasonable than the e-LEPS, MB1, and MB2 PESs. So the quasiclassical trajectory dynamic studies for the abstraction reaction, H′ + HBr → H′H + Br have been carried out on the ground-state MB3 PES in the present work. The details of the quasiclassical trajectory calculations are standard.[24,32,34,38] The QCT calculations have been performed for the collision energy range 0.1−2.6 eV, by running a batch of 5 × 10^5 trajectories. The integration step size in the trajectories was chosen to be 0.1 fs and the trajectories were initiated with an H′-HBr internuclear separation of 12.0 Å.

3. Results and Discussion

A. Cross Sections and Rotational-State Distributions of the Product. The comparison between the QCT-calculated integral cross sections in this work and previous QM-calculated integral cross section by Fu et al.[39] for the H′ + HBr(v=0,j=0) → H′H + Br reaction at the collision energy range of 0.1−2.6 eV is presented in Figure 2. The MB3 PES has been employed in both the current QCT calculation and the previous QM calculation. The QCT results reproduce quite satisfactorily the overall shape of the QM-calculated integral cross sections. There appear to be no significant quantum effects in the integral cross section calculations. Although zero-point energy (ZPE) leakage and tunneling play an important role in some reactions, such as the reactions O+OH and H+D_2,[40] they have little influence on the title abstraction reaction. The integral cross sections do not show an energy threshold as expected due to the very low barrier (only 0.066 eV) between reactants and products on the MB3 PES. As the collision energy increases, the reaction cross section rapidly reaches a maximum value at E_c = 0.8 eV and then decreases slowly, which agrees well with the previous investigations for the other homologous series of hydrogen atom abstraction reactions, such as the H + HCl abstraction reaction.[41]

Figure 3 shows a comparison of the QCT-calculated rotational distribution of the product H′H molecule on MB3 PES with the distribution from previous QCT calculations on an e-LEPS PES and from an experiment, for the chemical reaction H′ + HBr(v=0,j=0) → H′H(v'=2,j') + Br at E_c = 2.3 eV. The QCT-calculated rotational distributions of the product H′H molecule on the MB3 PES show nearly quantitative agreement with the experimental results. The product H′H rotational distributions on the MB3 PES have a preference for populating highly internally excited states compared with the experimental results. The present QCT calculation was carried out without considering the role of the spin statistics[42] in the scattering process. Due to the absence of the excited potential energy surface, only the ground potential energy surface was used in our calculation, which may explain the difference between the present QCT results and the experiment data. Another contribution to this

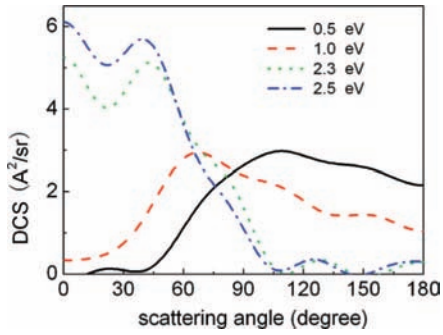

Figure 4. Total differential cross sections for H′ + HBr(v=0,j=0) → H′H + Br reaction at E_c = 0.5, 1.0, 2.3, and 2.5 eV, plotted as a function of scattering angle θ.

difference might be that MB3 PES underestimates the barrier height and acceptance cone for the abstraction reaction. This underestimation is also discussed by Fu et al. in their rate constant calculations for the abstraction reaction.[39] They found a larger theoretical rate constant by a factor of 2 for temperatures up to 550 K as compared with the experimental results. Hence, it is conceivable that the PES should be further improved to obtain better agreement between theory and experiment. On the basis of the QCT calculation for the title abstraction reaction on the e-LEPS PES, Zare and co-workers found that H′H products with low internal excitation are formed almost exclusively from direct trajectories that are nearly perfectly collinear at the transition state, whereas H′H products with high internal excitation are formed mainly from indirect trajectories having bent transition states.[12] So the characteristic of the PES in the region far away from the collinear geometry has a large influence on the dynamics of the title abstraction reaction. The barrier height for the title abstraction reaction for collinear geometry is 0.066 eV for the MB3 PES and 0.082 eV for the e-LEPS PES, whereas for the T-shaped geometry the barrier height is 0.916 and 0.799 eV, respectively. If the abstraction reaction is dominated by the nature of the PES at the collinear geometry, the QCT-calculated rotational-state-resolved cross sections on the MB3 PES should be larger than those on the e-LEPS PES. In fact the reverse results are obtained, which indicate that the characteristics of the PES in the region far away from the collinear geometry have a large influence on the title abstraction reaction dynamics. Therefore, some reaction trajectories do not follow the minimum energy reaction path at high collision energy and thus form H′H products with a broad rotational excited-state distribution at $v' = 2$. The discrepancies of the rotational-state-resolved cross sections obtained on the MB3 and e-LEPS PESs show that the indirect reactive trajectories play an important role in the product-state distribution for the title abstraction reaction H′ + HBr(v=0,j=0) → H′H(v'=2,j') + Br at high collision energy.

The differential cross sections (DCS) for the reaction at E_c = 0.5, 1.0, 2.3, and 2.5 eV are shown in Figure 4. At the low collision energy of 0.5 eV, the DCS shows broad backward-sideway distribution. When the collision energy increases, the angular distributions shift toward the forward direction. At the high collision energy of 2.5 eV, the most remarkable feature of the present DCS is the extremely peaked character in forward scattering directions with a tiny peak at a scattering angle of θ = 43°. Similar forward scattering was also found in previous QM calculations for the title abstraction reaction at E_c = 2.46 eV by Panda et al.[15] To study why these DCSs differ at different collision energies, the variants of internuclear distances H′—H, H—Br, and H′—Br, are presented as a function of propagation

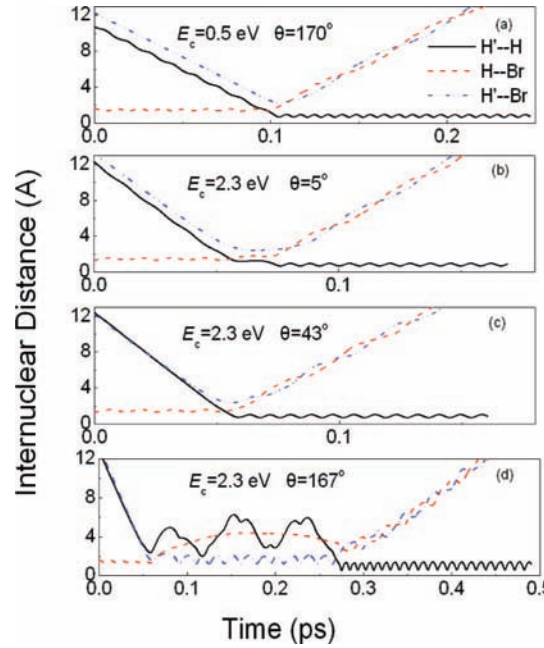

Figure 5. Internuclear distance of H′H, HBr, and H′Br as a function of propagation time, with a scattering angle of θ = 170° at E_c = 0.5 eV and 5°, 43°, and 167° at E_c = 2.3 eV.

time in Figure 5. The abstraction trajectories are selected randomly in scattering angle range of θ = 160−180° at E_c = 0.5 and θ = 0−5°, 43°, 160−180° at E_c = 2.3 eV. Parts a−c of Figure 5 show that the H′ atom collides with the HBr molecule and forms an H′H product that recoils away immediately. This is consistent with the direct reactive mechanism proposed by Zare and co-workers.[12] These trajectories come from the direct abstraction reactions and stay near the minimum energy reaction path. At low collision energies, the light H′H product with small momentum can recoil back easily from the heavy Br atom. When the collision energy is high enough, the light H′H product with high internal energy can move with little or no interference from the heavy Br atom in the same direction as the reagent H atom. This explains why we observed the dominance of forward scattering at high collision energies of 2.3 and 2.5 eV. The backward/sideways angular distributions at E_c = 0.5 eV and forward distributions at E_c = 2.3 and 2.5 eV can thus be considered as typical for trajectories that stay near the minimum energy reaction path. Zare and co-workers also proposed a distinct indirect reactive mechanism[12] for the title abstraction reactions that stay far from the minimum energy reaction path. The discrepancies between Figure 5a−c and Figure 5d show clear evidence of the two distinct reactive mechanisms. For these indirect abstraction collisions, the attacking H′ atom can approach to the HBr molecule from a very wide range of angles and suffer more than one collision before it migrates round to meet the other H atom. Figure 5d shows that the H′ atom undergoes three collisions with the HBr molecule before the H′H product is formed. Most of the scattering angles for these indirect abstraction reactions with more than one collision are located in the range from 160° to 180°, at a collision energy of 2.3 eV. But at a low collision energy of 0.5 eV, we did not observe indirect collisions. Although we observed indirect reactive trajectories at high collision energies, the indirect reactive mechanism has almost no influence on DCS. The DCSs for title abstraction reaction are mainly governed by the direct reactions whenever the collision energy is low or high.

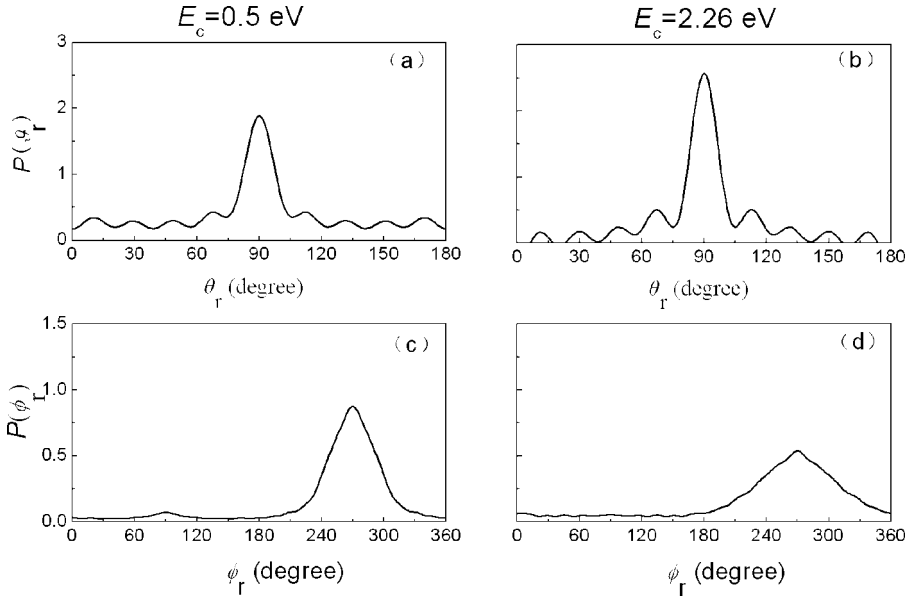

Figure 6. Rotational polarization of the H′H product from the H′ + HBr(v=0,j=0) → H′H + Br reaction at E_c = 0.5 and 2.3 eV. (a), (b) Distribution of $P(\theta_r)$ reflecting the **k**−**j′** correlation. (c), (d) Dihedral angle distribution of **j′**, $P(\phi_r)$, with respect to the **k**−**k′** plane.

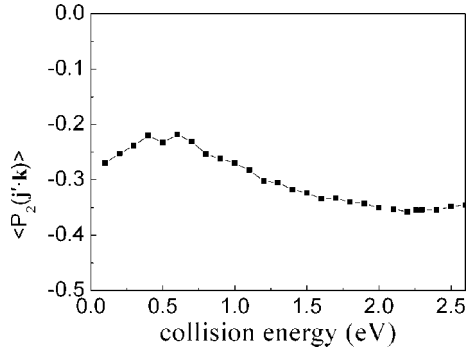

Figure 7. H′H product rotational alignment $\langle P_2(\mathbf{j'}\cdot\mathbf{k})\rangle$ for the reaction H′ + HBr(v=0,j=0) → H′H + Br as a function of collision energy.

B. Polarization of the Product. The distributions of $P(\theta_r)$ and $P(\phi_r)$ for the product H′H molecule from the H′ + HBr(v=0,j=0) → H′H + Br reaction are presented in Figure 6. The $P(\theta_r)$ distributions, describing the **k**−**j′** correlation, peak at θ_r angles close to 90° and are symmetric with respect to 90°, which demonstrates that **j′** is distributed with cylindrical symmetry in the product scattering frame and the direction of **j′** is preferentially perpendicular to **k** direction. The $P(\theta_r)$ distributions are very similar to the other homologous series of hydrogen atom abstraction reactions, such as the H + HCl abstraction reaction.[43] Because of the very low barrier on the ground-state MB3 PES for the title abstraction reaction, the rotational polarization of the product H′H molecule is very strong. The peak of the $P(\theta_r)$ distribution at E_c = 0.5 eV is lower than that at E_c = 2.3 eV, which means that the degree of the rotational alignment of the product H′H molecule increases as collision energy increases. This is also confirmed by the values of the product rotational alignment parameter $\langle P_2(\mathbf{j'}\cdot\mathbf{k})\rangle$ shown in Figure 7. The curve of $\langle P_2(\mathbf{j'}\cdot\mathbf{k})\rangle$ is in accord with the previous prediction for the light−heavy−light (LHL) mass combination by Han group.[37] The $\langle P_2(\mathbf{j'}\cdot\mathbf{k})\rangle$ values have a tiny peak at E_c = 0.4 eV and decrease lightly with increasing collision energy. As mentioned above, the indirect reactive mechanism has a remarkable influence on the title reaction dynamics, especially on the rotational-state distributions of the product H′H molecule. There are some reactive trajectories that do not follow the minimum energy reaction path at high collision energy, which are governed by an indirect reactive mechanism in which H′ suffers several collisions with the HBr molecule before the product H′H molecule is formed, as shown in Figure 5d. The indirect reactive trajectories linger for hundreds of femtoseconds in the translation state before forming the product H′H molecule, which is much longer than transition-state lifetimes of direct reactive trajectories. So the product rotational angular momentum has more time to lose memory of the initial angular momentum direction at high collision energies, which should lead to a weak degree of the product rotational alignment. However, the rotational alignment of the product H′H molecule is strong at high collision energy, which indicates that the effect of the indirect collisions on the product H′H rotational alignment is quite weak. So the influence of the direct reactions on the product H′H rotational alignment is dominant.

The dihedral angle distributions $P(\phi_r)$ shown in Figure 6c and d, describe **k**−**k′**−**j′** correlations. These $P(\phi_r)$ distributions tend to be asymmetric with respect to the **k**−**k′** scattering plane, directly reflecting the strong polarization of product rotational angular momentum. And the peak in the $P(\phi_r)$ distribution at ϕ_r angles close to 270° implies a preference for left-handed product rotation in planes parallel to the scattering plane. Of course, the little peak at ϕ_r angles close to 90° indicates a preference for the right-handed product rotation. We will use the term "in-plane" to refer to this preference of product molecule rotation in planes parallel to the scattering plane, and the term "out-of-plane" to refer to the preference of product molecule rotating in planes perpendicular to the scattering plane at the same time. The peaks of $P(\phi_r)$ that appear at ϕ_r = 90° and 270° show that **j′** is aligned preferentially along y-axis of the CM frame. The peak at ϕ_r = 270° is apparently stronger than that at ϕ_r = 90°, which means that **j′** tends to be oriented along the negative direction of the y-axis at the low collision energy of 0.5 eV. At the high collision energy of 2.3 eV, the peak at 270° becomes lower, which implies that the product rotational polarization is weakened, while the peak becomes broader, which indicates that the product molecule rotation has a preference of changing from the in-plane reaction mechanism to the out-of-plane mechanism. As mentioned above, the indirect collisions lead the H′ atom to undergo more than one collision

with the HBr molecule before the product H′H molecule is formed, which allows the product to have a long time to adjust to the rotational direction at high collision energies, as shown in Figure 5d. So, product molecule rotation has a preference for changing from the in-plane reaction mechanism to the out-of-plane mechanism when the collision energy increases. Obviously, the distribution of $P(\phi_r)$ is very sensitive to the indirect reactions at high collision energies.

4. Conclusion

We carried out a quasiclassical trajectory dynamic study for the abstraction reaction H′ + HBr(v=0,j=0) → H′H + Br on the MB3 potential energy surface. The integral cross sections, state-resolved rotational distributions, and product polarization for the abstraction reaction have been calculated for a collision energy range from 0.1 to 2.6 eV. The QCT-calculated integral cross sections are in good agreement with earlier QM results, and the state-resolved rotational distributions in $v' = 2$ at a collision energy of 2.3 eV show nearly quantitative agreement with the experimental results. The differences of the QCT-calculated rotational-state-resolved cross sections on the MB3 and e-LPES PESs show that the characteristics of the PES in the region far away from the collinear geometries have a large influence on the abstraction reaction dynamics. So some reactions do not follow the minimum energy reaction path at high collision energies and form product the H′H molecule with a broad rotational excited-state distribution at $v' = 2$. However, the indirect reactive mechanism has almost no influence on the total differential cross sections, which are mainly governed by the direct reactions at both low and high collision energies. The influence of the indirect reactions on the product rotational alignment are negligible, whereas the distribution of $P(\phi_r)$ is sensitive to the indirect reactions at high collision energies. The polarization of the product rotational angular momentum is weakened at high collision energies and the rotation of the product molecule has a preference for changing from the in-plane reaction mechanism to the out-of-plane mechanism.

Acknowledgment. The authors are very grateful to Professor Y. Kurosaki for providing the MB3 PES. This work was supported by the National Natural Science Foundation of China (Grant No. 10604012) and SRF for ROCS, SEM (2006).

References and Notes

(1) Neumark, D. M.; Wodtke, A. M.; Robinson, G. N.; Haygen, C. C.; Lee, Y. T. Phys. Rev. Lett. 1984, *54*.
(2) Castillo, J. F.; Manolopoulos, D. E.; Stark, K.; Werner, H. J. *J. Chem. Phys.* **1996**, *104*, 6531.
(3) Yao, L.; Han, K. L.; Song, H. S.; Zhang, D. H. *J. Phys. Chem. A* **2003**, *107*, 2781.
(4) Peterson, K. A.; Dunning, T. H. *J. Phys. Chem. A* **1997**, *101*, 6280.
(5) Yang, B. H.; Tang, B. Y.; Yin, H. M.; Han, K. L.; Zhang, J. Z. H. *J. Chem. Phys.* **2000**, *113*, 7182.
(6) Xie, T. X.; Zhang, Y.; Zhao, M. Y.; Han, K. L. *Phys. Chem. Chem. Phys.* **2003**, *5*, 2034.
(7) Chu, T. S.; Zhang, Y.; Han, K. L. *Int. Rev. Phys. Chem.* **2006**, *25*, 201.
(8) Mitchell, T. J.; Gonzalez, A. C.; Benson, S. W. *J. Phys. Chem.* **1995**, *99*, 16960.
(9) Umemoto, H.; Wada, Y.; Tsunashima, S.; Takayanagi, T.; Sato, S. *Chem. Phys.* **1990**, *143*, 333.
(10) Seakins, P. W.; Pilling, M. J. *J. Phys. Chem.* **1991**, *93*, 3.
(11) Picconatto, C. A.; Srivastava, A.; Valentini, J. J. *J. Chem. Phys.* **2001**, *114*, 1663.
(12) Pomerantz, A. E.; Camden, J. P.; Chiou, A. S.; Ausfelder, F.; Chawla, N.; Hase, W. L.; Zare, R. N. *J. Am. Chem. Soc.* **2005**, *127*, 16368.
(13) Townsend, D.; Lahankar, S. A.; Lee, S. K.; Chambreau, S. D.; Suits, A. G.; Zhang, X.; Rheinecker, J.; Harding, L. B.; Bowman, J. M. *Science* **2004**, *306*, 1158.
(14) Zhang, J. M.; Camden, J. P.; Brunsvold, A. L.; Upadhyaya, H. P.; Minton, T. K.; Schatz, G. C. *J. Am. Chem. Soc.* **2008**, *130*, 8896.
(15) Panda, A. N.; Althorpe, S. C. *Chem. Phys. Lett.* **2007**, *439*, 50.
(16) Aker, P. M.; Germann, G. J.; Valentini, J. J. *J. Chem. Phys.* **1989**, *90*, 4795.
(17) Lynch, G. C.; Truhlar, D. G.; Brown, F. B.; Zhao, J. G. *J. Phys. Chem.* **1995**, *99*, 207.
(18) Quan, W. L.; Song, Q.; Tang, B. Y. *Chem. Phys. Lett.* **2007**, *437*, 165.
(19) Quan, W. L.; Tang, P. Y.; Tang, B. Y. *Int. J. Quantum Chem.* **2008**, *107*, 657.
(20) Quan, W. L.; Song, Q.; Tang, B. Y. *Chem. Phys. Lett.* **2007**, *442*, 228.
(21) Kurosaki, Y.; Takayanagi, T. *J. Chem. Phys.* **2003**, *119*, 7838.
(22) Kurosaki, Y.; Takayanagi, T. *Chem. Phys. Lett.* **2005**, *406*, 121.
(23) Kurosaki, Y.; Takayanagi, T. Private communication.
(24) Chen, M. D.; Han, K. L.; Lou, N. Q. *J. Chem. Phys.* **2003**, *118*, 4463.
(25) Wang, M. L.; Han, K. L.; He, G. Z. *J. Chem. Phys.* **1998**, *109*, 5446.
(26) Wang, M. L.; Han, K. L.; He, G. Z. *J. Phys. Chem. A* **1998**, *102*, 10204.
(27) Gonzalez, M.; Sierra, J. D.; Francia, R.; Sayos, R. *J. Phys. Chem. A* **1997**, *101*, 8.
(28) Chen, M. D.; Tang, B. Y.; Han, K. L.; Lou, N. Q.; Zhang, J. Z. H. *J. Chem. Phys.* **2003**, *118*, 6852.
(29) Chen, M. D.; Tang, B. Y.; Han, K. L.; Lou, N. Q. *Chem. Phys. Lett.* **2001**, *337*, 349.
(30) Case, D. A.; Herschbach, D. R. *Mol. Phys.* **1975**, *30*, 1537.
(31) Case, D. E.; McClelland, G. M.; Herschbach, D. R. *Mol. Phys.* **1978**, *35*.
(32) McClelland, G. M.; Saenger, K. L.; Valentini, J. J.; Herschbach, D. R. *J. Phys. Chem.* **1979**, *83*, 947.
(33) Barnwell, J. D.; Loeser, J. G.; Herschbach, D. R. *J. Phys. Chem.* **1983**, *87*, 6.
(34) Truhlar, D. G.; Muckerman, J. T. Atom-Molecule Collision Theory, Plenum: New York, 1979.
(35) Shaferray, N. E.; Orrewing, A. J.; Zare, R. N. *J. Phys. Chem.* **1995**, *99*, 7591.
(36) Brouard, M.; Lambert, H. M.; Rayner, S. P.; Simons, J. P. *Mol. Phys.* **1996**, *89*, 403.
(37) Han, K. L.; He, G. Z.; Lou, N. Q. *J. Chem. Phys.* **1996**, *105*, 8699.
(38) Han, K. L.; He, G. Z.; Lou, N. Q. *Chin. Chem. Lett.* **1993**, *4*, 517.
(39) Fu, B.; Zhang, D. H. *J. Phys. Chem. A* **2007**, *111*, 9516.
(40) Varandas, A. J. C. *Chem. Phys. Lett.* **2007**, *439*, 386.
(41) Brownsword, R. A.; Kappel, C.; Schmiechen, P.; Upadhyaya, H. P.; Volpp, H. R. *Chem. Phys. Lett.* **1998**, *289*, 241.
(42) Chao, D. S.; Harich, S. A.; Dai, D. X.; Wang, C. C.; Yang, X. M.; Skodje, R. T. *J. Chem. Phys.* **2002**, *117*, 8341.
(43) Chen, M. D.; Han, K. L.; Lou, N. Q. *Chem. Phys.* **2002**, *283*, 463.

JP8105716